Isotope Geochemical Analysis of Strontium in Conodont Apatite: Implications for Global Cooling and the Timing of the Middle Ordovician Knox Unconformity

Undergraduate Research Thesis

Presented in Partial Fulfillment of the Requirements for graduation "with Honors Research Distinction in Earth Sciences" in the undergraduate colleges of The Ohio State University

by

Connor Bloomfield

The Ohio State University

December 2014

Project Advisor: Professor Matthew Saltzman, Department of Earth Sciences

Table of Contents

Abstract

The Middle Ordovician was characterized by marked temperature fluctuations, episodic global lowering of sea level, one of the largest biodiversification events in the fossil record, and a precipitous drop in oceanic $^{87}Sr/^{86}Sr$. This study examines the relationships among these factors via geochemical analysis and $^{87}Sr/^{86}Sr$ age dating of conodonts at the Knox Unconformity at East River Mountain, West Virginia. The East River Mountain data were correlated with counterparts from Knox Unconformity outcrops at Rocky Gap in Virginia and Clear Spring in Maryland. Results give an estimate of 5 Ma for the duration of the Knox Unconformity, and suggest it is composed of multiple unconformities. These unconformities are contemporaneous with seismic activity and regressions found in China and Baltoscandia, suggesting the Knox Unconformity was formed as a result of both tectonic activity and lowering of global sea level. Analysis in this paper suggests that the coinciding of regressions, biodiversification, and oceanic $^{87}Sr/^{86}Sr$ fall makes the possibility of relations amongst all these factors quite plausible. However, there is insufficient evidence to link them with Middle Ordovician temperature trends.

Introduction

Paleoclimate indicators are valuable tools for investigating how the Earth's environment has changed during its existence. One method widely utilized throughout the geologic record to study variations in temperature, an integral component of understanding climate, involves tracking changes in isotopic compositions of oxygen ($\delta^{18}O$) in marine fossils over time. This temperature proxy is particularly reliable in conodonts, an eel-like fossil that proliferated throughout the world's oceans from the Cambrian (beginning 541.0 Ma) through the Triassic (ending 201.3 Ma). $\delta^{18}O$ analysis has provided evidence for significant cooling in the Paleozoic era's Middle Ordovician (470.0 to 458.4 Ma), the primary time interval of focus in this study (Trotter, 2008; see Figure 1).

This cooling coincided with the Great Ordovician Biodiversification Event (GOBE), one of the largest episodes of species origination in the fossil record (Trotter, 2008). The aforementioned cooling and GOBE occurred amongst a reduction in the $^{87}Sr/^{86}Sr$ ratio of the global oceans (Young et al., 2009). Decreasing $^{87}Sr/^{86}Sr$ is thought by Young et al. to be a direct result of increased weathering of young volcanic material, which injects proportionally more ^{86}Sr into oceans. This surge in weathering arises from increased mountain building and convergent plate boundary activity, situations which are conducive to both volcanism and breaking down lithic material. The causal link between enhanced weathering of young volcanics (basaltic composition) and a cooling climate is based on the fact that basaltic minerals have a relatively high percentage of calcium ions that can combine with atmospheric CO_2 to sequester this greenhouse gas as $CaCO_3$ (carbonate) rock (Berner, 2006). However, the nature of the relationship of a cooling

climate and GOBE with the fall in $^{87}Sr/^{86}Sr$, and the implied associated orogenic activity, is unclear because of uncertainty in precisely dating each of these events (Young et al., 2009). Furthermore, the evidence for cooling based on $\delta^{18}O$ studies (Trotter et al., 2008) is controversial because the oxygen isotopic composition of the oceans can be affected by factors other than temperature (Finnegan et al., 2011).

I address this issue of the relationship amongst these factors via geochemical analysis of the Appalachian Basin's Middle Ordovician Knox Unconformity (Mussman and Read, 1986; Dwyer and Repetski, 2012), which may be an indicator of eustatic sea level drop, cooling of the climate and ice buildup independent of $\delta^{18}O$.

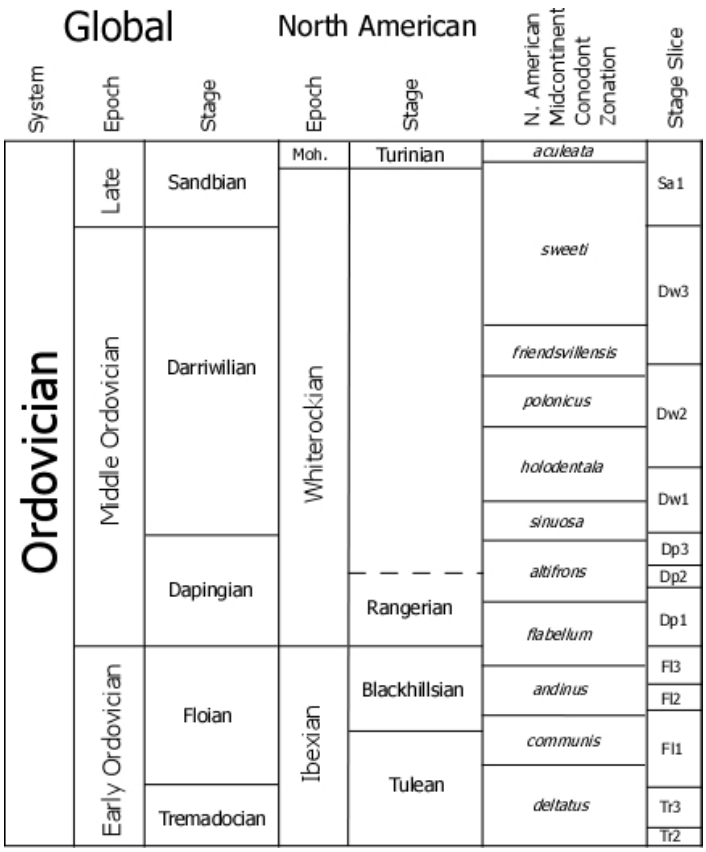

Figure 1: Time scale of focus in this study (Dwyer and Repetski, 2012).

Figure 2: Sample locality for Knox Unconformity rocks processed in this study (Google Earth).

Goals and Objectives

Determining the duration, age, and cause of the Knox Unconformity is the primary goal of this study. This unconformity represents a period of erosion and non-deposition, typical of a drop in sea level; however, it is not certain whether the unconformity represents a eustatic (global) drop in sea level due to ice sheet buildup or a local drop in sea level related to the uplift of the Appalachian Mountains (Mussman and Read, 1986). If significant cooling occurred during the Middle Ordovician, then the formation of ice sheets would be observable as a lowering of sea level in the stratigraphic record in the Appalachian Basin and elsewhere around the world. The first step in testing the hypothesis of a global sea level drop is to date accurately the observed sea level events in various regions of the world and compare their timing (Haq and Schutter, 2008). I explore these relationships in this paper by dating the Knox Unconformity through geochemical processing and analysis of conodont apatite and then comparing this timing to sea level events in China and Baltoscandia (e.g., Lin et al., 2012; Goldman et al., 2014).

Previous Work

Age correlation using $^{87}Sr/^{86}Sr$ is based on the fact that the isotopic ratio of Sr dissolved in Earth's oceans has changed over geologic time in response to weathering of rocks of different age and composition (i.e., older, granitic rocks generally have more radiogenic Sr than younger basaltic rocks due to decay of Rb through time). This relationship of ^{87}Sr to ^{86}Sr has been measured from the Precambrian to the Quaternary (McArthur et al., 2012). At any point in the geologic record, $^{87}Sr/^{86}Sr$ was homogeneous in the planet's oceans. This is because Sr's oceanic residence time is approximately 2-4 Ma, much longer than the ~1000 yr oceanic mixing time (Elderfield, 1986; Palmer and Edmond, 1989; Veizer, 1989; McArthur, 1994; Davis et al., 2003).

Dating using Sr isotope stratigraphic (SIS) is performed by comparing $^{87}Sr/^{86}Sr$ trends of undated samples to those of known biostratigraphic (relative) or geochronologic (absolute) age. Due to the uniformity of $^{87}Sr/^{86}Sr$ in the oceans, only samples of marine minerals are measured for Sr isotopic composition. Their maritime origins result in providing reliable archives of $^{87}Sr/^{86}Sr$ in the oceans, the only locale in which Sr isotopic composition is homogeneous (McArthur et al., 2012). Conodonts are among the marine fossils most utilized for Ordovician biostratigraphy, and the tooth-like apatite elements of this eel-like marine organism are used in this study for $^{87}Sr/^{86}Sr$ measurements (Saltzman et al., 2014).

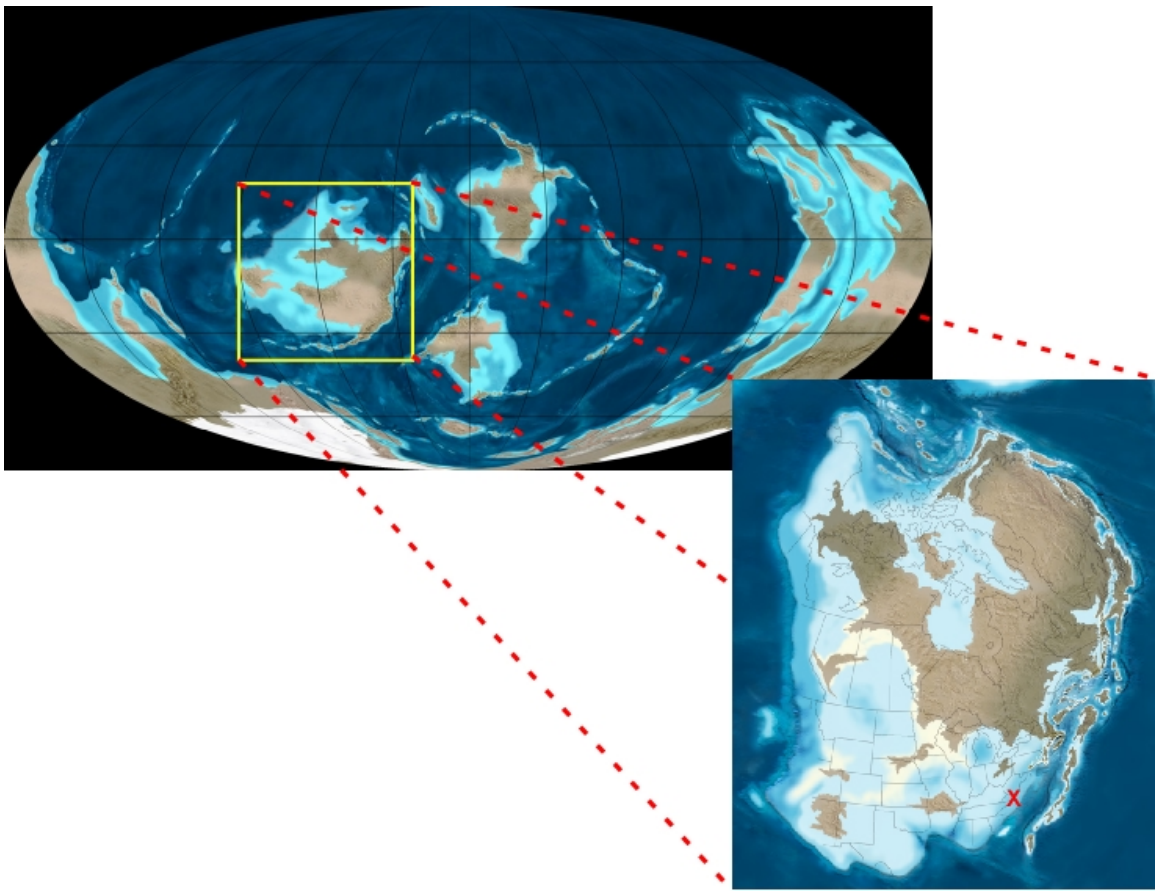

Figure 3: Paleogeographic map of the Middle Ordovician, with Laurentia highlighted by yellow and magnified. The sample locality of East River Mountain is marked with an "X" on the Laurentia map. Maps produced by Dr. Ron Blakey (http://www.cpgeosystems.com/470moll.jpg ; http://www.cpgeosystems.com/namO470.jpg).

Methods

The specimens used in this study's geochemical analysis of the Knox Unconformity were collected from an outcrop near the East River Mountain Tunnel by Nick Umholtz. The rocks, including mixed carbonates and siliciclastics originating from the West Virginia side of the Tunnel, include a total of five samples. Samples, approximately two kg each, were broken down with use of a rock crusher to increase surface area and thus accelerate the subsequent dissolving steps. After processing through the rock crusher, samples were placed in a formic acid solution (6%) buffered with $CaCO_3$ and $Ca(PO_4)_3$. Samples were left in this buffered solution until at least half of the rock had dissolved, which took three to seven days. The resultant solution was sieved to isolate 0.125-0.250 mm residue, which was subsequently desiccated overnight at 150°C with use of an oven. The dried residue was then passed through magnets to remove hematite, magnetite, and other magnetic oxides. This non-magnetic leftover residue underwent heavy liquid separation in acetylene tetrabromide, was rinsed with acetone, and left overnight.

With use of a microscope and paintbrush, the resultant residue was scoured for conodonts lacking both mineral overgrowths and evidence of alteration (see Figure 4 for model photos of the conodonts). To remove non-apatite material from the fossils, the conodonts were rinsed with 1 mL of 18 Ω Milli-Q water, sonicated, and left overnight. Conodonts were afterwards pretreated in buffered 1 M ammonium acetate (pH 8). Pretreated samples were then dissolved in 6 N HCl, spiked with an ^{84}Sr tracer, and purified with use of a H^+ cation exchange resin through two elutions of 2 N HCl in glass columns.

To measure the $^{87}Sr/^{86}Sr$ ratio in the conodont apatite, samples were processed through a Finnigan MAT multicollector thermal ionization mass spectrometer in the Radiogenic Isotope Laboratory at The Ohio State University (separation and spectromety procedures of Foland and Allen, 1991).

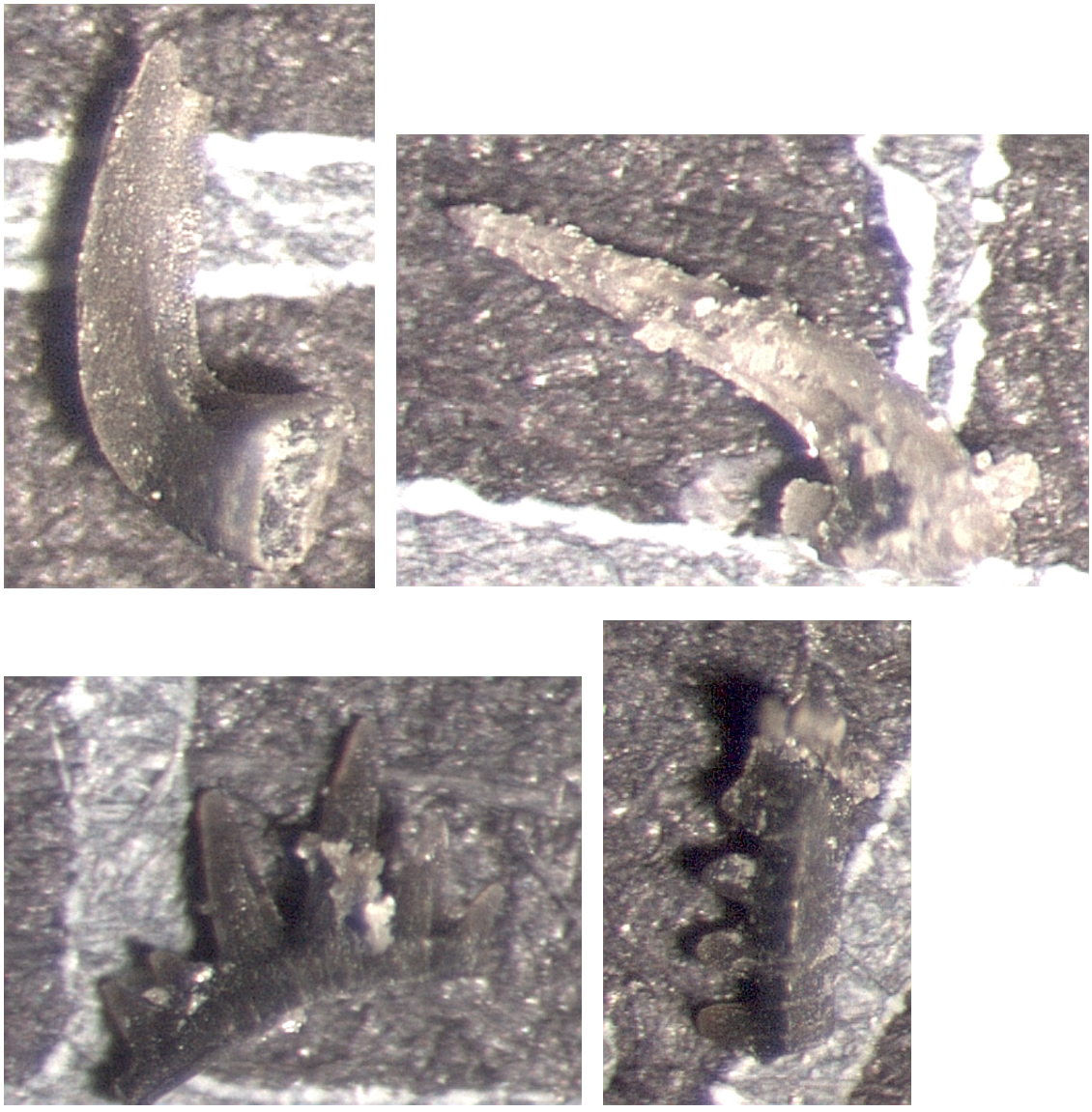

Figure 4: Representative pictures of conodonts. The top conodonts are from KN-500, and are *Glyptoconus quadraplicatus*. The bottom conodonts are from KN-4500, and are *Plectodina aculeata*.

Results

Of the five rock samples processed and scoured for conodonts (Sr-bearing apatite), three (KN-500, KN-1500, and KN-4500) were productive. The conodont species in both KN-500 and KN-1500 were identified as *Glyptoconus quadraplicatus* (conferred Ji and Barnes, 1994), while those in KN-4500 were *Plectodina aculeata* (conferred Sweet, 1982).

Only KN-500 and KN-4500 resulted in a sufficient quantity of conodont apatite for measurement of $^{87}Sr/^{86}Sr$. The mass spectrometer measured an $^{87}Sr/^{86}Sr$ value of 0.708891 for KN-500, which is stratigraphically below the Knox Unconformity. A $^{87}Sr/^{86}Sr$ measurement of 0.708309 was obtained for KN-4500, which is above the Unconformity. The uncertainty for the $^{87}Sr/^{86}Sr$ values of KN-500 and KN-4500 is $1.4x10^{-5}$ and $1.0x10^{-5}$, respectively.

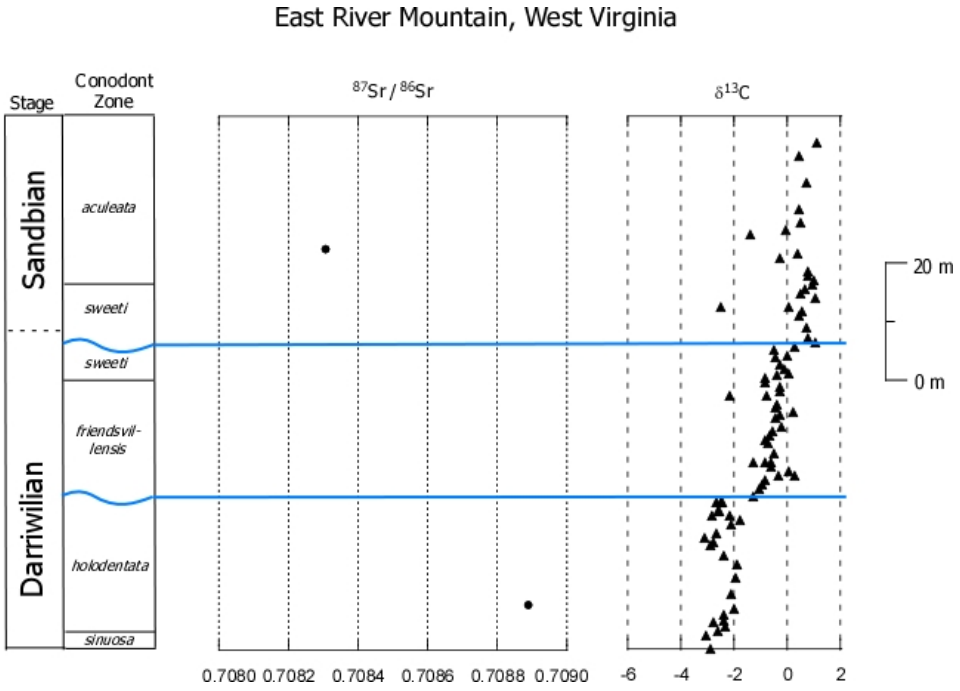

Figure 5: East River Mountain conodont $^{87}Sr/^{86}Sr$ data plotted alongside known $\delta^{13}C$ values (Umholtz, N., 2014). The blue lines represent inferred unconformities.

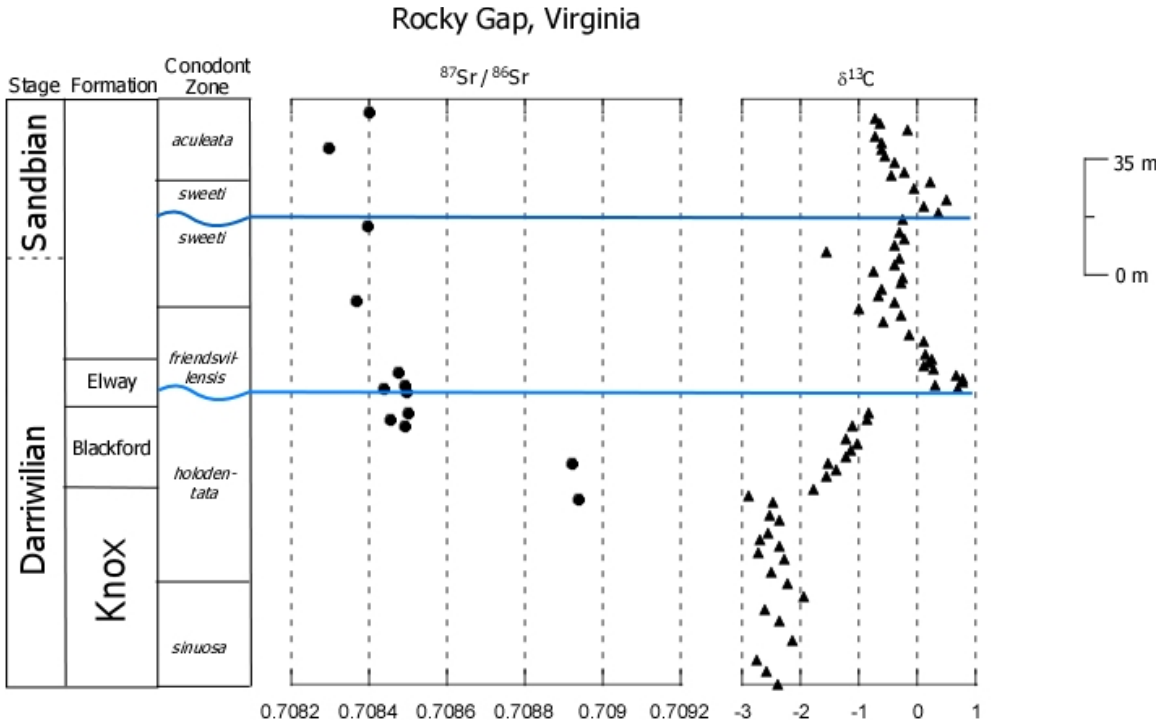

Figure 6: Conodont $^{87}Sr/^{86}Sr$ and $\delta^{13}C$ data from Rocky Gap, 8 miles from East River Mountain (Edwards et al., 2014). The blue lines represent inferred unconformities.

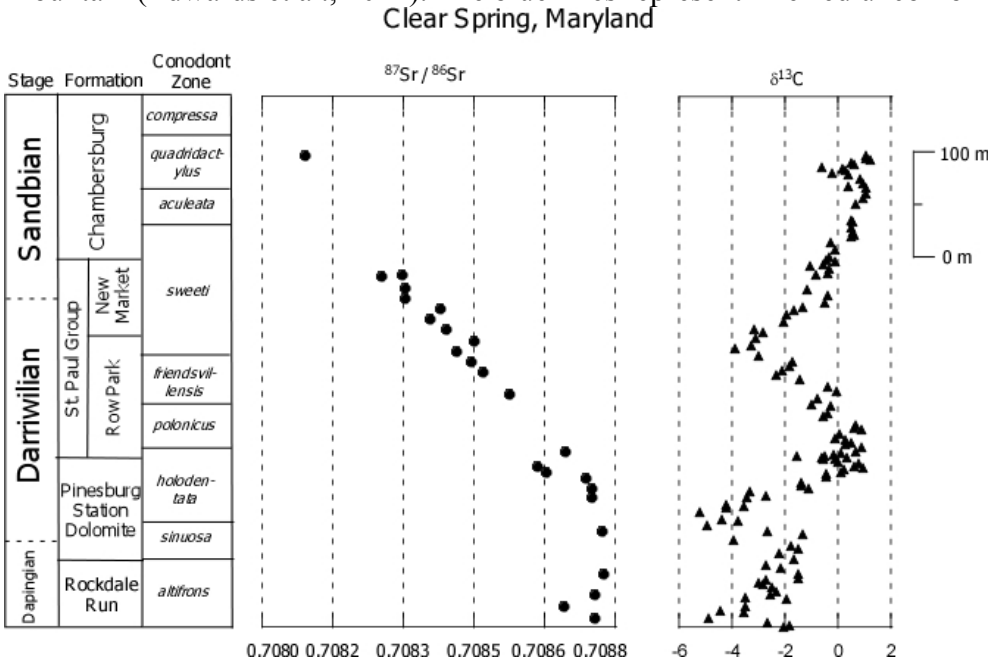

Figure 7: $^{87}Sr/^{86}Sr$ and $\delta^{13}C$ data from Maryland's Clear Spring (Saltzman and Thomas, 2012; Saltzman et al, 2014). This served as the reference for calibration of the Rocky Gap and East River Mountain sections in this study.

Discussion

Dating the Knox Unconformity

The Knox Unconformity $^{87}Sr/^{86}Sr$ ratios were correlated with use of East River Mountain $\delta^{13}C$ data and Saltzman et al.'s (2014) $^{87}Sr/^{86}Sr$ and $\delta^{13}C$ values for Clear Spring (Saltzman and Thomas, 2012). $\delta^{13}C$ is used as a tool for correlating rocks in a manner similar to Sr isotope stratigraphy, reflecting the long residence time of carbon relative to the mixing time of the oceans (Berner, 1990). Further correlation with $^{87}Sr/^{86}Sr$ and $\delta^{13}C$ data from Rocky Gap, 8 miles from the East River Mountain sample locality, helped in dating the Unconformity (Edwards et al., unpublished). See Figure 6 for a graphical explanation of this correlation.

Correlation suggests that sample KN-500, which lies below the Unconformity, was deposited shortly after the transition between the *H. sinuosa* and *H. holodentata* conodont zones in the Dapingian Stage of the Middle Ordovician (Fig. 1). This corresponds to a numeric age of approximately 466.5 Ma. Sample KN-4500, above the unconformity, appears to have deposited in the beginning *P. aculeata* conodont zone in the Sandbian Stage. The numeric age of this sample correlates to about 456.5 Ma. The temporal gap between KN-500 and KN-4500, around 10 Ma, represents an estimate of the duration of the Knox Unconformity at East River Mountain.

Conodont biostratigraphy, calculations of carbonate dissolution rates, and observed karst relief at the Knox Unconformity suggest a duration of hundreds of thousands of years to 10 Ma, dependent on the locality (Mussman and Read, 1986; Dwyer and Repetski, 2012). The 10 Ma determined using $^{87}Sr/^{86}Sr$ correlation in this study is thus plausible on the older end of estimates, and represents a maximum for the

temporal extent of the Knox Unconformity. Indeed, the lack of results from intermediate samples representing the long range between KN-500 and KN-4500 suggests the 10 Ma determined in this study is not an accurate representation of the amount of time missing in the Unconformity because of the 40 m stratigraphic gap between the two samples. The East River Mountain correlated time scale (Figure 5) shows the two unconformities represent a total gap of 5 Ma, compared to the previous 10 Ma estimate. This means that between KN-500 and KN-4500 lies 5 Ma of geologic time recorded in 40 m of strata, resulting in an estimated deposition rate of 8 m of rock every million years.

Causes of the Knox Unconformity

The formation of the Knox Unconformity has been attributed to eustatic (global) sea level fall, convergent plate activity, and to a combination of both eustatic and tectonic forces. The Unconformity's far-reaching extent across much of eastern North America supports the eustatic origination hypothesis, since a sea level drop (glacio-eustasy) would have a more geographically extensive impact than would a convergent boundary (Mussman and Read, 1986; Dwyer and Repetski, 2012).

The Early to Middle Ordovician were host to a series of short-term global decreases in sea level of over 60 m (Haq and Schutter, 2008; see Figure 7 for a graphical display of Ordovician sea levels). The coincidence of these eustatic sea level drops with the timing of the Knox Unconformity in the Appalachian Basin could support the eustatic origination hypothesis. Contemporaneous unconformities caused in part by regression are found in the Tarim Basin in northwest China's Xinjiang Uyghur Autonomous Region (Lin et al., 2012). More specifically, two of these regressions

occurred at 458.2 Ma and 460.9 Ma, during the timeframe of the Knox Unconformity (Lin et al., 2012). Both of these Tarim Basin regressions have coeval counterparts in other parts of the world as documented by Haq and Schutter (2008).

Goldman et al. (2014) noted comparatively low sea levels in the Middle and Upper Ordovician from approximately 472 to 463 Ma and again from 461 to 458 Ma. These regressions took place at the same time as those observed by Lin et al. (2012) in the Tarim Basin, and overlap with the 466.5 to 456.5 Ma lifetime of the East River Mountain Knox Unconformity determined in this study. Since eustasy helped form unconformities in other parts of the world around the same time as the formation of the Knox Unconformity, it is likely sea level affected the development of the Unconformity. Furthermore, the presence of various regressions during the time period of the Unconformity's formation suggests it did not form as a result of a single sea level lowering, but rather from multiple eustatic drops. The presence of multiple regressions, thus suggesting more than one unconformity, as observed and diagrammed in Figures 3 and 4 supports this notion of the Knox Unconformity being composed of a series of unconformities and possibly multiple episodes of cooling and ice sheet buildup.

However, the Knox Unconformity's role as the demarcation between passive margin and foreland basin convergent margin depositional facies suggests tectonic forces may have also influenced its development. As the North American continental margin collided with a magmatic arc during the Middle Ordovician, eastward subduction may have passed over a peripheral bulge (Mussman and Read, 1986). The continental margin's travel over this peripheral bulge could have caused a warp producing as much as 183 m of uplift (Jacobi, 1981). The resultant relative sea level fall would have exposed

the continental margin to sub-aerial or aerial erosional processes, producing an unconformity. The time at which the Knox Unconformity began coincides with the occurrence of the aforementioned convergent boundary collision, shortly before or during the Whiterockian Stage (Mussman and Read, 1986; Dwyer and Repetski, 2012). This coinciding of the Knox Unconformity's commencement with the Ordovician collision makes the possibility of tectonic forces in the Unconformity's development quite plausible.

The presence of both tectonic and eustatic forces forming the Knox Unconformity is not mutually exclusive. Rather, the preponderance of evidence for sea level fall and convergent boundary activity suggests both were instrumental its production (Dwyer and Repetski, 2012).

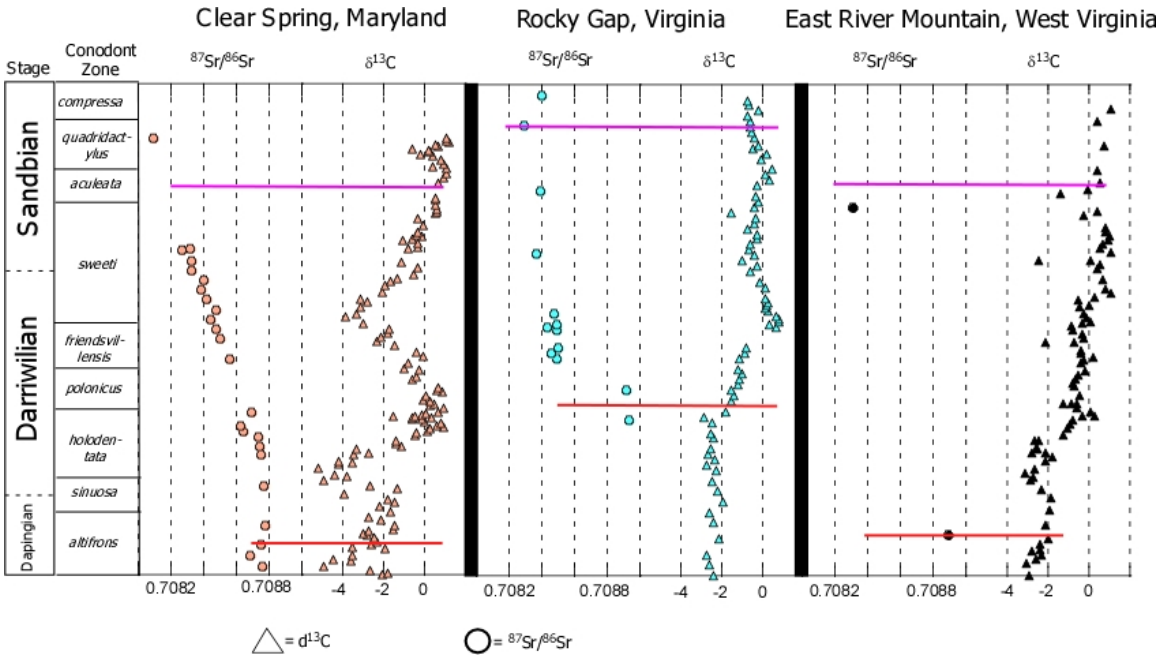

Figure 8: Visual demonstration of calibration of Rocky Gap and East River Mountain sections using Clear Spring data as a reference. Lines of the same color are contemporaneous, and serve as the basis for calibration of the East River Mountain data. The three sections are not shown to scale. Stage and conodont zone information in this figure is only applicable to Clear Spring.

Causes and Implications of Decreasing $^{87}Sr/^{86}Sr$

The drop in $^{87}Sr/^{86}Sr$ from before to after the Knox Unconformity at East River Mountain (from ~0.7089 to ~0.7083) occurred amongst a larger and more prolonged lowering throughout much of the Ordovician. This isotopic Sr ratio drop, from ~0.7090 to ~0.7078, greatly accelerated beginning in the Darriwilian and ended in the Katian (Young et al, 2009).

^{86}Sr enters the ocean via weathering of non-radiogenic volcanic materials, resulting in a decrease in $^{87}Sr/^{86}Sr$. Increased weathering can be caused by higher rates of seafloor spreading and resultant upsurges in mountain building, which allow more materials to be eroded. $^{87}Sr/^{86}Sr$ can also drop due to eustatic rise and submersion of sources of radiogenic ^{87}Sr in old granitic continental interiors (Young et al., 2009).

The presence of a K-bentonite stratigraphically above the Knox Unconformity supports the notion that weathering of volcanics helped cause the observed $^{87}Sr/^{86}Sr$ drop (Leslie et al., 2012). The volcanic material may have originated from the eastern Laurentia island-arcs formed with the Taconic Orogeny (Young et al., 2009).

The weathering of volcanics would normally cause a decrease in average global temperature, as the calcium ions of the volcanics combine with atmospheric CO_2 to produce carbonate rock. This carbonate rock, $CaCO_3$, acts as a sink for the greenhouse gas CO_2, resulting in global cooling (Berner, 2006). However, as shown in Figure 9, the findings of this study suggest the Knox Unconformity occurred amidst rising global temperatures. Young et al. (2009) account for this contradiction by suggesting that during this time period the climate effects of increased weathering of volcanics were offset by volcanic outgassing, which injected more CO_2 into the atmosphere. In the late Katian,

when volcanic weathering rates were still high and volcanic outgassing had returned to baseline levels, the average global temperature dropped greatly (Young et al., 2009).

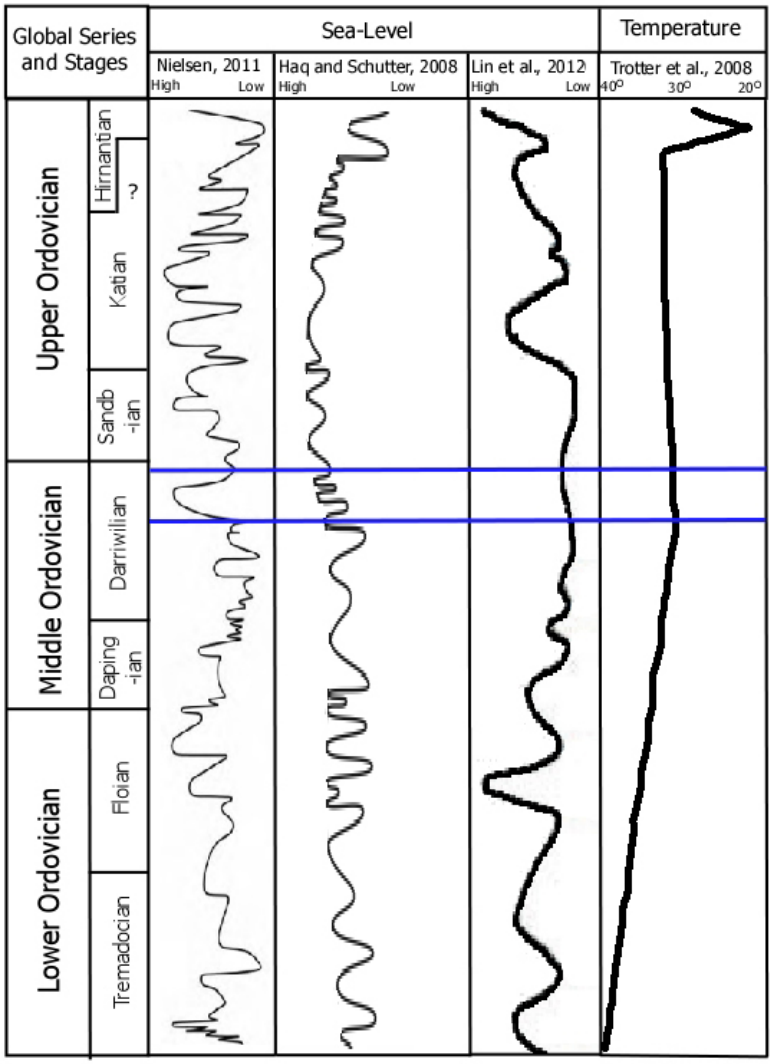

Figure 9: Sea level curves modeling the entire Ordovician. The blue lines represent the regressions attributed in this paper to helping cause the formation of the Knox Unconformity.

Conclusion

The 10 Ma duration estimate for the Knox Unconformity from conodont biostratigraphy and $^{87}Sr/^{86}Sr$ dating correlation conforms to results of previous studies (Dwyer and Repetski, 2012). However, the 40 m stratigraphic gap between samples in this study suggests this overestimates the duration Unconformity at East River Mountain. Thus, the 5 Ma estimate which accounts for rock deposition rates is likely more accurate.

The presence of both global regressions and plate activity during the timeframe of the Knox Unconformity lends credence to the notion that both eustatic and tectonic forces are responsible for its creation. Additionally, the presence of multiple regressions during the Knox Unconformity suggests it is composed of multiple unconformities rather than a single large one.

The coeval occurrence of regressions, the GOBE, and oceanic $^{87}Sr/^{86}Sr$ fall makes the possibility of relations amongst these quite plausible (Trotter et al., 2008; Young et al, 2009). However, further research is needed to clarify the extent and nature of such links, especially with regards to the relationship between these factors and temperature.

Suggestions for Future Work

A more precise estimate of the duration of the Knox Unconformity via $^{87}Sr/^{86}Sr$ dating could be obtained in subsequent studies through a higher sampling rate. Such an improvement could be achieved by acquiring a larger numbers of rock samples. This would increase the likelihood of finding conodonts, and thus $^{87}Sr/^{86}Sr$ data, consequently improving the resolution of dating efforts. A greater resolution would further support efforts at understanding the regional geologic record by examining more deeply the various regressions that together constitute the Knox Unconformity.

Investigations into the varying durations of the Knox Unconformity across multiple, distant North American outcrops could be of additional scholarly benefit. Such research, combined with other studies on contemporaneous sea levels, tectonic activity, and paleogeography, could help determine the balance between eustasy and plate activity in formation of the Unconformity. The results of this work could further elucidate the relationship between sea level and plate tectonics in regressions and the formation of unconformities, providing a deeper understanding of how such factors influence the recording of events in the geologic record.

There are still considerable gaps in the knowledge of conodonts in the Appalachian Mountains. Additional analysis, classification, and study of Appalachian conodonts could aid in regional biostratigraphy, as well as provide more knowledge of past environmental and evolutionary trends.

Acknowledgments

I am extremely grateful to Dr. Cole Edwards for his extensive and patient instruction in conodont sample processing. Thank you to Jeff Linder for providing a practical working knowledge of preparing and operating the mass spectrometer. A further acknowledgment of thanks is given to Nick Umholtz for providing rock samples from the Knox Unconformity as well as discussion relevant to this work. Dr. Stig Bergstrom was invaluable in his lending of materials and time to help identify the conodonts found in the rock samples. I would also like to deeply thank Dr. Matt Saltzman for taking time out of his busy schedule to guide and support the completion of this endeavor.

References

Berner, R.A., 1990, Atmospheric carbon dioxide levels over Phanerozoic time: Science, vol. 249, p.1382-1386.

Berner, R. A., 2006, Inclusion of the weathering of volcanic rocks in the GEOCARBSULF model: American Journal of Science, v. 306, p. 295-302, doi:10.2475/05.2006.01.

Blakey, R., Middle Ordovician (470Ma) Mollewide plate tectonic map, digital image, http://www.cpgeosystems.com/470moll.jpg (accessed October 2014).

Blakey, R., Middle Ordovician (470Ma) North American paleogeographic map, digital image, http://www.cpgeosystems.com/namO470.jpg (accessed October 2014).

Davis, A.C., Bickle, M.J., and Teagle, D.A.H., 2003, Imbalance in the oceanic strontium budget: Earth and Planetary Science Letters, vol. 211, no. 1-2, p. 173-187, doi:10.1016/S0012-821X(03)00191-2.

Dwyer, G.S., and Repetski, J.E., 2012, The Middle Ordovician Knox Unconformity in the Black Warrior Basin, *in* Derby, J.R., Fritz, R.D., Longacre, S.A., Morgan, W.A., and Sternbach, C.A., eds., The Great American Carbonate Bank: The Geology and Economic Resources of the Cambrian-Ordovician Sauk Megasequence of Laurentia, Volume 98: AAPG and Shell, p. 345-56, doi:10.1306/13331498M983499.

Edwards, C.T., Saltzman, M.R., Leslie, S.A., Bergström, S.M., Sedlacek, A.R.C., Howard, A., Bauer, J.A., Sweet, W.C., Young, S.A., 2014, Strontium isotope ($^{87}Sr/^{86}Sr$) stratigraphy of Ordovician bulk carbonate: Implications for preservation of primary seawater values: Geological Society of America Bulletin (in press).

Elderfield, H., 1986, Strontium isotope stratigraphy: Palaeogeography, Palaeoclimatology, Palaeoecology, v. 57, no. 1, p. 71-90, doi:10.1016/0031-0182(86)90007-6.

Finnegan, S., Bergmann, K., Eiler, J.M., Jones, D.S., Fike, D.A., Eisenman, I., Hughes, N.C., Tripati, A.K., and Fischer, W.W., 2011, The magnitude and duration of Late Ordovician-Early Silurian glaciation: Science, v. 331, no. 6019, p. 903-906, doi:10.1126/science.1200803.

Foland, K.A, and Allen, J.C, 1991, Magma sources for Mesozoic anorogenic granites of the White Mountain magma series, New England, USA: Contributions to Mineralogy and Petrology, vol. 109, p. 195-211.

Goldman, D., Bergström, S.M., Sheets, H.D., and Pantle, C., 2014, A CONOP9 composite taxon range chart for Ordovician conodonts from Baltoscandia: A framework for biostratigraphic correlation and maximum-likelihood biodiversity analyses: GFF, v. 136, no. 2, p. 342-54, doi:10.1080/11035897.2013.809549.

Haq, B. U., and Schutter, S.R., 2008, A chronology of Paleozoic sea-level changes: Science, v. 322, no. 5898, p. 64-68. doi:10.1126/science.1161648.

Jacobi, R.D., 1981, Peripheral bulge—a causal mechanism for the Lower/Middle Ordovician Unconformity along the western margin of the Northern Appalachians: Earth and Planetary Science Letters, v. 56, p. 245-251, doi:10.1016/0012-821X(81)90131-X.

Ji, Z., and Barnes, C.R., 1994, Lower Ordovician Conodonts of the St. George Group, Port Au Port Peninsula, Western Newfoundland, Canada: Calgary, Canadian Society of Petroleum Geologists, 149 p.

Leslie, S., Sell, B., Saltzman, M., Repetski, J., and Edwards, C., 2012, The East River Mountain K-bentonite bed, a Central Appalachian marker that closely approximates the Middle-Upper Ordovician (Darriwilian-Sandbian) boundary, presentation at the Geological Society of America Abstracts with Programs, vol. 44, no. 7, p. 590.

Lin, C., Yang, H., Liu, J., Rui, Z., Cai, Z., Li, S., and Yu, B., 2012, Sequence architecture and depositional evolution of the Ordovician carbonate platform margins in the Tarim Basin and its response to tectonism and sea-level change: Basin Research, v. 24, no. 5, p. 559-582, doi:10.1111/j.1365-2117.2011.00536.x.

McArthur, J.M., 1994, Recent trends in strontium isotope stratigraphy: Terra Nova, vol. 6, no. 4, p. 331-358, doi:10.1111/j.1365-3121.1994.tb00507.x.

McArthur, J. M., Howarth, R.J., and Shields, G.A., 2012, Strontium isotope stratigraphy, *in* Gradstein, F.M., ed., The Geologic Time Scale 2012, Volume 1 (first edition): Amsterdam, Elsevier Science, p. 127-144, doi:10.1016/B978-0-444-59425-9.00007-X.

Mussman, W. J., and Read, J.F., 1986, Sedimentology and development of a passive- to convergent-margin unconformity: Middle Ordovician Knox Unconformity, Virginia Appalachians: Geological Society of America Bulletin, vol. 97, no. 3, p. 282-295, doi:10.1130/0016-7606(1986)972.0.CO;2.

Nielsen, A.T., 2011, A re-calibrated sea-level curve for the Ordovician of Baltoscandia, *in* Webby, B., Paris, F., Droser, M.L., and Pervical, I., eds., Ordovician of the World: 11th Ordovician Symposium on the Ordovician System: Madrid, Madrid Instituto Geológico y Minero de España 14, p. 399-401.

Palmer, M.R., and Edmond, J.M., 1989, The strontium isotope budget of the modern ocean: Earth and Planetary Science Letters, vol. 92, no. 1, p. 11-26, doi:10.1016/0012-821X(89)90017-4.

Saltzman, M. R., and Thomas, E., 2012, Carbon isotope stratigraphy, *in* Gradstein, F.M., ed., The Geologic Time Scale 2012, Volume 1 (first edition): Amsterdam, Elsevier Science, p. 207-232, doi:10.1016/B978-0-444-59425-9.00011-1.

Saltzman, M.R., Edwards, C.T., Leslie, S.A., Dwyer, G.S., Bauer, J.A., Repetski, J.E., Harris, A.G., and Bergström, S.M., 2014, Calibration of a conodont apatite-based Ordovician $^{87}Sr/^{86}Sr$ curve to biostratigraphy and geochronology:

Implications for Stratigraphic Resolution: Geological Society of America Bulletin, vol. 126, no. 11-12, p. 1551-1568.

Sweet, W.C., 1982, Conodonts from the Winnipeg Formation (Middle Ordovician) of the Northern Black Hills, South Dakota: Journal of Paleontology, v. 56, no. 5, p. 1029-1049.

Trotter, J.A., Williams, I.S., Barnes, C.R., Lecuyer, C., and Nicoll, R.S., 2008, Did cooling oceans trigger Ordovician biodiversification? Evidence from conodont thermometry: Science, v. 321, no. 5888, p. 550-54, doi:10.1126/science.1155814.

Umholtz, N.M., 2014, Middle to Late Ordovician ∂^{13}C and 87Sr/86Sr stratigraphy in Virginia and West Virginia: Implications for the timing of the Knox unconformity [M.S. thesis]: Columbus, Ohio State University, 55 p.

Veizer, J., 1989, Strontium isotopes in seawater through time: Annual Review of Earth and Planetary Sciences, vol. 17, p. 141-167, doi:10.1146/annurev.ea.17.050189.001041.

Young, S.A., Saltzman, M.R., Foland, K.A., Linder, J.S., and Kump, L.R., 2009, A major drop in seawater 87Sr/86Sr during the Middle Ordovician (Darriwilian): Links to volcanism and climate?: Geology, v. 37, no. 10, p. 951-54, doi:10.1130/G30152A.1.

37°17'3.99"N And 81° 7'30.80"W. Google Earth. October 2012. October 15, 2014.

Appendix

Sr Data

Sample name	Sr ppm	$^{87}Sr/^{86}Sr$	Uncertainty	Conodont mass (g)
KN-500	15397	0.708891	0.000014	$3.2x10^{-4}$
KN-4500	8676	0.708309	0.000010	$8.2x10^{-4}$

Rock Sample Data

Sample name	Sample mass (kg)
KN-500	1.50
KN-1500	0.45
KN-2500	0.70
KN-3500	1.00
KN-4500	1.40